ResearchGate

See discussions, stats, and author profiles for this publication at: https://www.researchgate.net/publication/231235715

Composition and Microstructure of Cobalt Oxide Thin Films Obtained from a Novel Cobalt(II) Precursor by Chemical Vapor Deposition

ARTICLE · JANUARY 2001

CITATIONS
41

READS
280

2 AUTHORS, INCLUDING:

Davide Barreca
National Research Council, Padova
289 PUBLICATIONS **4,290** CITATIONS

SEE PROFILE

Available from: Davide Barreca
Retrieved on: 26 January 2016

Composition and Microstructure of Cobalt Oxide Thin Films Obtained from a Novel Cobalt(II) Precursor by Chemical Vapor Deposition

Davide Barreca and Cristian Massignan

Dipartimento di Chimica Inorganica, Metallorganica ed Analitica, Università di Padova, Via Loredan 4, I-35131 Padova, Italy

Sergio Daolio and Monica Fabrizio

Istituto di Polarografia ed Elettrochimica Preparativa, CNR, Corso Stati Uniti 4, I-35020 Padova, Italy

Clara Piccirillo

High Vacuum Process, Via Azzoni 3b, I-43100 Parma, Italy

Lidia Armelao and Eugenio Tondello*

Centro di Studio sulla Stabilità e Reattività dei Composti di Coordinazione del CNR, Via Marzolo 1, I-35131 Padova, Italy

Received March 20, 2000. Revised Manuscript Received October 31, 2000

The present work reports the synthesis and the characterization of cobalt oxide thin films obtained by chemical vapor deposition (CVD) on indium tin oxide (ITO) substrates, using a cobalt(II) β-diketonate as precursor. The complex is characterized by electron impact mass spectrometry (EI-MS) and thermal analysis in order to investigate its decomposition pattern. The depositions are carried out in a cold wall reactor in the temperature range 350−500 °C at different oxygen pressures, to tailor film composition from CoO to Co_3O_4. The crystalline nanostructure is evidenced by X-ray diffraction (XRD), while the surface and in-depth chemical composition is studied by X-ray photoelectron (XPS) and X-ray excited auger electron spectroscopy (XE-AES). Atomic force microscopy (AFM) is employed to analyze the surface morphology of the films and its dependence on the synthesis conditions. Relevant results concerning the control of composition and microstructure of Co−O thin films are presented and discussed.

Introduction

Materials based on cobalt oxides have attracted a great interest in view of their potential applications in scientific and technological fields.[1−3] Co_3O_4, the most stable phase in the Co−O system, is a mixed valence compound [$Co^{II}Co^{III}_2O_4$] with a normal spinel structure. Cobalt oxide-based materials have received attention for the production of solid-state sensors[4,5] and heterogeneous catalysts[6−8] and as intercalation compounds for energy storage.[9−11]

One of their most important applications is the preparation of electrochromic devices (ECDs)[12] exploiting the reversible changes of their optical properties under an external electrical stimulus.[13] Co_3O_4 has been used as an active material for its color change from brown to light yellow when Li^+ ions are inserted;[14] the corresponding electrochromic efficiency is relatively high ($\approx$25 $cm^2 \cdot C^{-1}$). (The electrochromic efficiency is defined as $\Delta OD(\lambda)/Q$, where Q is the injected charge ($C \cdot cm^{-2}$) producing the absorbance variation ΔOD for a given λ). Besides, cobalt monoxide is often used as a counter electrode because of its anodic coloration properties.[12,15,16]

* Corresponding author: E-mail: tondello@chin.unipd.it. Phone: +39-0498275220. Fax: +39-0498275161.

(1) Jiménez, V. M.; Fernández, A.; Espinós, J. P.; González-Elipe, A. R. *J. Electron Spectrosc. Relat. Phenom.* **1995**, *71*, 65.
(2) Hamada, H.; Haneda, M.; Kakuta, N.; Miura, H.; Inomi, K.; Nanba, T.; Qi Hua, W.; Veno, A.; Ohfune, H.; Udagawa, Y. *Chem. Lett.* **1997**, 887.
(3) Tanaka, M.; Mukaia, M.; Fujimuri, Y.; Kondoh, M.; Tasaka, Y.; Baba, H.; Usami, S. *Thin Solid Films* **1996**, *281−282*, 453.
(4) Ando, M.; Kobayashi, T.; Iijima, S.; Harita, M. *J. Mater. Chem.* **1997**, *7*, 1779.
(5) Yamaura, H.; Tamaki, J.; Moriya, K.; Miura, N.; Yamazoe, N. *J. Electrochem. Soc.* **1997**, *144*, L158.
(6) Nkeng, P.; Koening, J.; Gautier, J.; Chartier, P.; Poillerat, G. *J. Electroanal. Chem.* **1996**, *402*, 81.
(7) Weichel, S.; Møller, P. J. *Surf. Sci.* **1998**, *399*, 219.
(8) Okamoto, Y.; Imanaka, T.; Teranishi, S. *J. Catal.* **1980**, *65*, 448.
(9) Ramachandram, K.; Oriakhi, C. O.; Lerner, M. M.; Koch, V. R. *Mater. Res. Bull.* **1996**, *31*, 767.
(10) Hutchins, M. G.; Wright, P. J.; Grebenik, P. D. *Solar Energy Mater.* **1987**, *16*, 113.
(11) Barrera, E.; Gonzales, I.; Viveros, T. *Sol. Energy Mater. Sol. Cells* **1998**, *51*, 69.
(12) Svegl, F.; Orel, B.; Hutchins, M. G.; Kalcher, K. *J. Electrochem. Soc.* **1996**, *143*, 1532.
(13) Granquist, C. G. In *Handbook of Inorganic Electrochromic Materials*; Elsevier Science: Amsterdam, 1995.
(14) Maruyama, T.; Arai, S. *J. Electrochem. Soc.* **1996**, *143*, 1383.

10.1021/cm001041x CCC: $20.00 © 2001 American Chemical Society
Published on Web 01/17/2001

Such a broad perspective of utilization has increased the importance of the synthesis procedure. In particular, nanotextured materials with a high surface-to-volume ratio are extremely interesting for advanced applications, since they are expected to have superior functional properties. Different methods have been employed for the preparation of Co−O-based thin films, such as PLD (pulsed laser deposition),[3] RF sputtering,[17] electrodeposition,[10,11] magnetron sputtering,[18] spray pyrolysis,[4,6,19] plasma oxidation,[20] electron-beam evaporation,[21] and sol−gel processes.[22] Among the various synthesis techniques, CVD offers many advantages since it allows an accurate tailoring of the system composition, microstructure, and morphology by a suitable choice of the precursor compound and the deposition conditions. CVD of Co_3O_4 has been carried out only by $Co(OAc)_2$ (OAc = acetate),[23] $Co(acac)_2$ (Hacac = 2,4-pentanedione),[14,24] and $Co(NO_3)_3$[25] as precursor compounds. The first two precursors have been used for CVD of pure CoO thin films, with a strictly controlled, low-oxygen atmosphere.[26,27]

This paper reports the CVD of cobalt oxide thin films with controlled composition by means of a Co(II) β-diketonate, $Co(dpm)_2$ (Hdpm = 2,2,6,6-tetramethyl-3,5-heptanedione) as a novel precursor. The use of a Co(II) complex, instead of the commercial $Co(dpm)_3$, enables the deposition of CoO and/or Co_3O_4 from the same precursor only by changing the O_2 content in the reaction atmosphere. This complex was stable as a monomer because each β-diketonate ligand with bulky *tert*-butyl substituents occupied two coordination sites of the metal;[28] it also had an appreciable volatility (vaporization already at 90 °C). Moreover, the Co−O bonds were thermally labile, favoring the removal of the volatile byproducts in oxidizing atmosphere. The absence of Co−C bonds reduced the possibility of C contamination of the films. Besides, this compound was relatively stable to air and moisture and could be easily prepared and purified. Film depositions have been performed on indium−tin oxide (ITO), a transparent conductor, considering its possible application in all-solid-state electrochromic devices.

This paper describes the compositional and microstructural features of the films, highlighting the influence of the reaction atmosphere on the precursor decomposition mechanism.

Experimental Section

Synthesis and Characterization of $Co(dpm)_2$. The precursor was synthesized by following a modification of a procedure previously proposed.[29] A solution of the β-diketone sodium salt was prepared by adding the Hdpm ligand to a solution of NaOH. The resulting liquid was mixed with a solution of $Co(OAc)_2 \cdot 4H_2O$ (Merck, 99%) previously prepared. The compound was thus recovered by precipitation and purified by a vacuum sublimation (120 °C, 10^{-2} mbar) until its melting point fell in the range 140−144 °C[30] (yield for the complete synthesis = 60%). The dark-violet powder could be easy manipulated in air and has been characterized by ^{1}H NMR, FT-IR, and Vis−NIR spectroscopies, together with elemental analysis. Electron impact mass spectrometry (EI-MS) and thermogravimetric analysis (TGA) have been employed for preliminary investigations of its decomposition pattern.

Anal. Found: C, 61.1; H, 9.0. Calcd for $C_{22}H_{38}O_4Co$: C, 62.1; H, 9.0.

Precursor mass spectra were obtained using a single-focus magnetic instrument VG-MS16 (mass resolution = 5000) under standard electron ionization conditions (E_1 = 70 eV). This analysis revealed that the precursor was a relatively stable molecular compound ($M^{+\bullet}/z$ = 425, 40%) and that it decomposed easily through the loss of the *tert*-butyl groups ($[M^{+\bullet} - (CH_3)_3C]/z$ = 368, 100%). The peak at m/z = 184 (5%) was attributed to the β-diketone Hdpm, while the loss of the *tert*-butyl groups was confirmed by the signal at m/z = 127 ($[(CH_3)_3C-CO-CH_2^-CO]^{+\bullet}$, 9%). Finally, the peak at m/z = 242 (20%) arose from the molecular ion ($M^{+\bullet}/z$ = 425) by the loss of a β-diketonate ligand. These data indicated a clean fragmentation pattern for $Co(dpm)_2$. The precursor TGA (TG-S2 thermobalance, Perkin-Elmer, 8 °C/min heating rate) showed its complete evaporation in a single step (weight loss ca. 98.6%) with the onset at 160 °C and atmospheric pressure.

Film Deposition. The films were deposited in a cold-wall low-pressure CVD reactor with a resistively heated susceptor. O_2 was used as carrier and reactive gas for both the oxide synthesis and the removal of organic ligands as oxidized volatile byproducts. The precursor was placed in a vaporization vessel connected to the reactor tube and maintained at 90 °C throughout each film deposition. The gas line and valves between the bubbler and the reaction tube were heated to avoid condensation of the precursor. The pressure was measured by a capacitance manometer, and the gas flow was controlled by a mass-flow controller. The ITO substrate (indium tin oxide, In_2O_3:Sn, ρ = 10 Ω/square)[12,23] was deposited by sputtering on glass (film thickness = 60 nm, Sn = 1.2 at. %). Before CVD, the substrates were degreased in soap−water, washed in water and in isopropyl alcohol, and finally dried in air. To minimize the carbon contamination, their surfaces were heated in the reactor chamber by flowing O_2 for 40 min. The deposition conditions are reported in Table 1. Film thickness (Table 1) was measured by means of a profilometer (Tencor P-10 profiler, Tencor).

X-ray Diffraction. XRD analyses were performed using a Philips PW 1820 diffractometer (Cu Kα radiation, 40 kV, 50 mA) equipped with a thin film attachment (glancing angle = 0.5°). The Debye−Scherrer equation was used to determine the average crystallite sizes.

X-ray Photoelectron Spectroscopy (XPS) and X-ray Excited Auger Electron Spectroscopy (XE-AES) Analyses. A Perkin-Elmer Φ 5600ci spectrometer with monochromatized Al Kα radiation (1486.6 eV) was used for the XPS and

(15) Monk, P. M. S.; Chester, S. L.; Higham, D. S.; Partridge, R. D. *Electrochim. Acta* **1994**, *39*, 2277.
(16) Kuwabara, K.; Ichikawa, S.; Sugiyama, K. *J. Mater. Sci.* **1987**, *22*, 4499.
(17) Cook, J. G.; van Der Meer, M. P. *Thin Solid Films* **1986**, *144*, 165.
(18) Dimitrov, D. V.; Hadjipanayis, G. C.; Papaefthymiou V.; Simopoulos, A. *IEEE Trans. Magn.* **1998**, *51*, 69.
(19) Singh, R. N.; Handani, M.; Koening, J.; Poillerat G.; Gautier, J. *J. Appl. Electrochem.* **1990**, *20*, 442.
(20) Koyano, G.; Watanabe, H.; Okuhara, T.; Misono, M. *J. Chem. Soc., Faraday Trans.* **1996**, *92*, 3425.
(21) Seike, T.; Nagai, J. *Sol. Energy Mater.* **1991**, *22*, 107.
(22) (a) El Baydi, M.; Poillerat, G.; Rehspringer, J.; Gautier, J. L.; Koening, J.; Chartier, P. *J. Solid State Chem.* **1994**, *109*, 281. (b) Lakshmi, B. B.; Patrissi, C. J.; Martin, C. R. *Chem. Mater.* **1997**, *9*, 2544.
(23) Maruyama, T.; Nakai, T. *Sol. Energy Mater.* **1991**, *23*, 25.
(24) Cheng, C. S.; Serizawa, M.; Sakata, H.; Hirayama, T. *Mater. Chem. Phys.* **1998**, *53*, 225.
(25) Colombo, D. G.; Gilmer D. C.; Young V. G.; Campbell S. A.; Gladfelter W. L. *Chem. Vap. Deposition* **1998**, *4*, 220.
(26) Gazzoli, D.; Occhiuzzi, M.; Cimino, A.; Cordischi, D.; Minelli G.; Pinzari, F. *J. Chem. Soc., Faraday Trans.* **1996**, *92*, 4567.
(27) (a) Fujii, E.; Tomazawa, A.; Fujii, S.; Torii, H.; Hattori M.; Takayama, R. *Jpn. J. Appl. Phys.* **1993**, *32*, L1448. (b) Fujii, E.; Torii, H.; Tomazawa, A.; Takayama R.; Hirao, T. *J. Mater. Sci.* **1995**, *30*, 6013.
(28) Cotton, F. A.; Soderberg, R. H. *J. Am. Chem. Soc.* **1962**, *84*, 872.
(29) (a) Ellern, J. B.; Ragsdale, R. O. *Inorg. Synth.* **1968**, *11*, 82. (b) Berg, E. W.; Herrera, N. M. *Anal. Chim. Acta* **1972**, *60*, 117.
(30) Cotton, F. A.; Wood, J. S. *Inorg. Chem.* **1964**, *3*, 245.

Table 1. Deposition Parameters, Thickness, and Phase Composition of the Cobalt Oxide Thin Films[a]

sample	substrate temp (°C)	tot pressure (mbar)	O_2 flow rate (sccm)	phases	av thickness (nm)	growth rate (nm min^{-1})
A	350	10	150	Co_3O_4	543 ± 10	7
B	400	10	150	Co_3O_4	413 ± 10	9
C	450	10	150	Co_3O_4	623 ± 13	10
D	500	10	150	Co_3O_4	726 ± 33	12
E	350	2	50	CoO	204 ± 10	3
F	400	2	50	CoO + Co_3O_4	261 ± 12	4
G	450	2	50	Co_3O_4	515 ± 30	13
H	500	2	50	Co_3O_4	1276 ± 39	21

[a] The precursor vaporization temperature was 90 °C. The uncertainty on the film thickness, calculated as the semidispersion of the average value, was indicative of the thickness homogeneity.

XE-AES measurements. The working pressure was lower than 10^{-7} Pa. The spectrometer was calibrated by assuming the binding energy (BE) of the Au $4f_{7/2}$ line at 84 eV with respect to the Fermi level. The detailed spectra of Co 2p, O 1s, C 1s, and Co LMM were recorded in the following conditions: pass energy 58.7 eV; 0.25 eV step^{-1}, 50 s step^{-1}, which correspond to resolution of 0.6 eV. After a Shirley-type background subtraction,[31] the raw spectra were fitted using a nonlinear least-squares fitting program adopting Gaussian−Lorentzian peak shapes for all the peaks. The atomic compositions were evaluated using sensitivity factors as provided by Φ V5.4A software.

Depth profiles of the different elements were carried out by Ar^+ sputtering at 2.5 kV and 0.4 mA·cm^{-2} beam current density, with an argon partial pressure of 5×10^{-8} Pa. All the samples were conducting enough to neglect charging effects.

Optical Absorption. The Vis−NIR absorption spectra of the films were recorded on a Cary 5E (Varian) UV−Vis−NIR dual-beam spectrophotometer, operating in transmittance mode at normal incidence.

Atomic Force Microscopy (AFM) Analysis. Images were taken using a Park Autoprobe CP instrument operating in contact mode in air. The background was subtracted from the images using the ProScan 1.3 software from Park Scientific.

Results and Discussion

To investigate the influence of the process parameters on film microstructure and composition (Table 1), two sample sets were prepared, differing for the O_2 total pressure and flow rate. All the films were homogeneous, crack-free, and well adherent to the substrate. While all the Co_3O_4 layers appeared bluish-brown and reflecting, the CoO-containing films (samples E and F) were yellow-gray.

Structural Analysis. The XRD spectra of the films deposited at $p = 10$ mbar were almost independent on the growth temperature. All these films contained the polycrystalline cubic Co_3O_4.[32] Even though a slight decrease of the (400) reflection intensity at $2\vartheta \approx 44.8°$ was observed on increasing the deposition temperature, the films showed no appreciable preferential orientation. Similar diffraction patterns were obtained for the samples G and H ($p = 2$ mbar), deposited at 450 and 500 °C respectively (Figure 1). Otherwise, sample E spectrum showed three weak peaks at $2\vartheta = 36.9$, 42.8, and 62°. These signals corresponded respectively to the (111), (200), and (220) reflections of cubic CoO.[33] Moreover, in this spectrum the ITO reflections are more visible because of the low crystallinity of the monoxide overlayer. The analysis of sample F spectrum was complicated by the copresence of both CoO and Co_3O_4. A first inspection showed only the three reflections

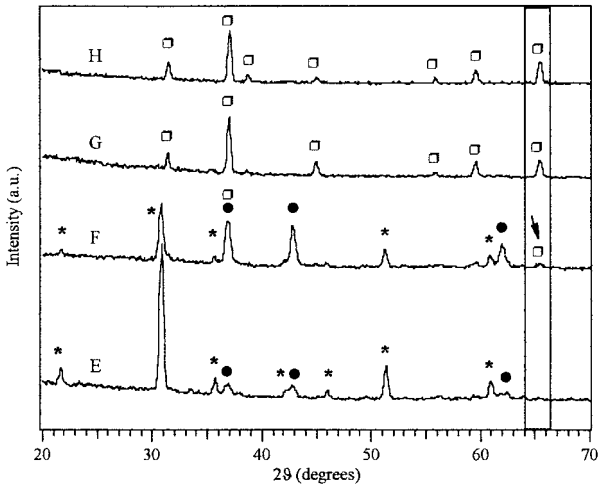

Figure 1. XRD patterns for the films synthesized at p = 2 mbar. The reflections labeled with an asterisk, ●, and □ are due to the ITO substrate, to CoO, and to Co_3O_4, respectively.

related to the CoO phase− (111), (200), and (220)−but a careful analysis revealed a weak peak at $2\vartheta = 65.5°$ (arrow in Figure 1), which was assigned to the (400) reflection of Co_3O_4,[32] as observed for samples G and H.

The peak at $2\vartheta = 37°$ in the pattern of sample F could therefore be attributed to both the (111) reflection of CoO and the (311) reflection of Co_3O_4.

The average crystallite sizes were estimated by applying the Debye−Scherrer equation to the most intense peak of the spectrum; the obtained values fell in the 13−28 nm range, indicating that all the films were nanotextured. The smallest crystallites (13 and 16 nm, F and E respectively) were evidenced on the CoO-containing films; this observation may be explained by the different growth kinetics of CoO and Co_3O_4 on the ITO surface. Since CoO was obtained only in mild conditions,[26,27] it was hypothesized that its formation from the vapor phase was slower than that of Co_3O_4, limiting the grain growth after the first nucleation stages. As a result, the average crystallite size was lower for the films containing CoO as the main phase.

Surface and In-Depth Analysis. The surface and in-depth chemical composition was investigated combining XPS and XE-AES techniques. It was in fact observed that the binding energy (BE) values of the most intense Co photoelectronic peak (Co 2p) did not allow a clear distinction between CoO [pure Co(II)] and Co_3O_4 [$Co^{II}Co^{III}{}_2O_4$]. In the last case, a single asymmetrical peak is usually evidenced since the contributions of the two oxidation states are not well resolved.[34] Therefore, the analysis of the AES peaks and the evaluation of the Auger parameter, calculated by the

(31) Shirley, D. A. *Phys. Rev.* **1972**, *55*, 4709.
(32) Pattern Nos. 42-1467 and 43-1003, JCPDS−ICDD, 1992.
(33) Pattern No. 43-1004, JCPDS−ICDD, 1992.

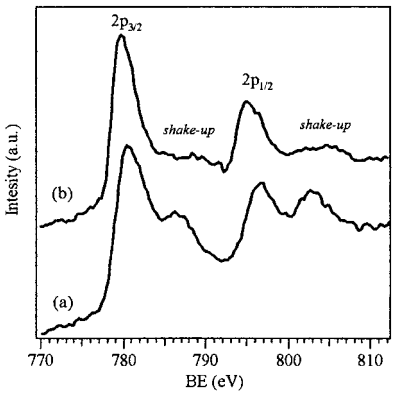

Figure 2. Co 2p XPS surface peaks for samples: (a) E (CoO); (b) D (Co_3O_4). Note that the shake-up satellites are much more intense for CoO than for Co_3O_4 samples.

sum of the Co $2p_{3/2}$ binding energy (BE) and the Co LMM Auger peak kinetic energy (KE), were essential to distinguish Co_3O_4 from CoO in the deposited samples.[35] Furthermore, the presence of pure CoO was confirmed by the intense shake-up satellites 6 eV above the primary spin−orbit BEs.[36]

On all sample surfaces only cobalt, oxygen, and carbon signals were detected; the absence of In signals confirmed the uniform coverage of the substrate surface. Excluding sample E, the Co 2p peak shape and position was similar for all the films. The Co $2p_{3/2}$ binding energy (≈780.0 eV, full width at half-maximum (FWHM) = 3.3 eV) and the Auger parameters (≈1553.2 eV) were in agreement with those previously reported for Co_3O_4,[36] confirming the presence of this oxide. A further indication of this result was the low intensity of the shake-up satellites at ≃9 eV from the main spin−orbit components[37] (Figure 2b). A different spectrum was recorded for sample E, obtained in mild oxidative conditions (T = 350 °C; p = 2 mbar). The Co $2p_{3/2}$ binding energy (≈780.4 eV, FWHM = 4.2 eV) was slightly higher than in the previous cases and the signal was characterized by intense shake-up peaks at ≃5.4 eV from the spin−orbit components (Figure 2a). These satellites were used as a fingerprint for the recognition of high-spin Co(II) species in CoO.[38] The presence of this oxide in sample E was further indicated by (i) the binding energy difference between the two components of the Co2p doublet (16 eV) and the FWHM of the Co $2p_{3/2}$ component, both greater than that of Co_3O_4 due to multiplet splitting and (ii) the Auger parameter (1554.2 eV) in agreement with literature data for CoO.[39] Nevertheless, the presence of small quantities of Co_3O_4 due to air exposure cannot be definitively ruled out.

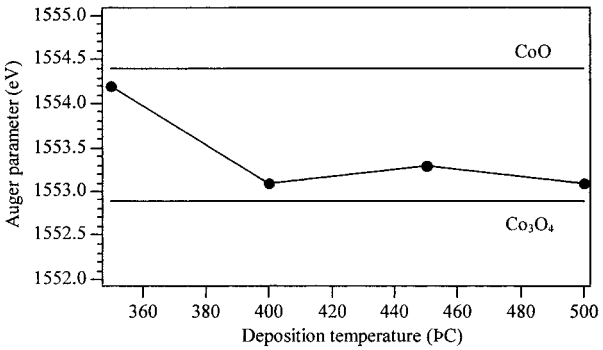

Figure 3. Dependence of the Auger parameter values on the deposition temperature for the films deposited at 2 mbar. The literature values for CoO and Co_3O_4 are shown for comparison.

Figure 3 reports the dependence of the Auger parameter from the deposition temperature for set 2 samples (p = 2 mbar). The decrease of the Auger parameter from 350 °C (sample E) to higher temperatures (samples F−H) indicated that the monoxide synthesis was favored at the lowest deposition temperatures.

The results of XPS and XE-AES spectroscopy were generally in agreement with the XRD data, excluding sample F. In fact the diffraction pattern of this film contained reflections due to both the oxides, whereas the XPS and XE-AES surface analyses detected only the presence of Co_3O_4. This disagreement could be explained supposing that, during the nucleation process, CoO was initially formed and subsequently partially converted into the most thermodynamically stable Co_3O_4 in the outer grain parts. Similar observations were reported in a previous work of the PE-CVD of cobalt oxides.[27b]

The presence of multiplet splitting in CoO and the coexistence of Co(II) and Co(III) in Co_3O_4, whose binding energies are reported to differ by 0.2−0.5 eV, constitute a serious problem in attempting spectral deconvolution of the Co $2p_{3/2}$ signal. In fact, the spectra of the single regions have been recorded with a resolution of 0.6 eV (see Experimental Section). Moreover, it is extremely difficult to obtain a reliable fitting in the case of Co_3O_4, since the relative percentages of Co(II) and Co(III) are influenced by the adopted fitting procedure.[36e] For these reasons, a significant spectral decomposition of the Co $2p_{3/2}$ signal could not be obtained.

The O 1s surface XPS peak for the Co_3O_4 containing films could be resolved in three different components. The first, at ≃529.6 eV (50.8−67.9%), was referred to the oxide.[40] The second and the third (≃531.2 and 532.3 eV, 31.3−23.1 and 17.9−9%, respectively) were attributed to the presence either of hydroxyl or carbonate species[36e,41] or of coordinative unsaturated oxygen, with a higher covalence degree in the Co−O bonds.[1] Since in the present case the intensity of the peak at 531.2 eV appeared dependent on air exposure, the contribution of −OH and CO_3^{2-} surface contaminants could not be ruled out. In the case of CoO sample, the O 1s signal could be fitted with three components at 529.5 (I,

(34) Strydom, C. A.; Strydom, H. J. *Inorg. Chim. Acta* **1989**, *159*, 191.
(35) Haber, J.; Ungier, L. *J. Electron Spectrosc. Relat. Phenom.* **1977**, *12*, 305.
(36) (a) McIntyre, N. S.; Cook, M. G. *Anal. Chem.* **1975**, *47*, 2208. (b) Oku, M.; Hirokawa, K. *J. Electron Spectrosc. Relat. Phenom.* **1976**, *8*, 475. (c) Ramsey, M. G.; Russell, G. J. *Appl. Surf. Sci.* **1985**, *22/23*, 206. (d) Shen, Z. X.; Allen, J. W.; Lindberg, P. A. P.; Dessau, D. S.; Wells, O. B.; Borg, A.; Ellis, W.; Kang, J. S.; Oh, S. J.; Lindau, I.; Spicer, W. E. *Phys. Rev. B* **1990**, *42*, 1817. (e) Tyuliev, G.; Angelov, S. *Appl. Surf. Sci.* **1988**, *32*, 381.
(37) Jiménez, V. M.; Espinós, J. P.; González-Elipe, A. R. *Surf. Interface Anal.* **1998**, *26*, 62, and references therein.
(38) McIntyre, N. S.; Johnston, D. D.; Coatsworth, L. L.; Davidson, R. D.; Brown, J. R. *Surf. Interface Anal.* **1990**, *15*, *265*.
(39) (a) Khawaja, E. E.; Durrani, S. M. A.; Al-Adel, F. F.; Salim, M. A.; Sakhawat Hussain, M. *J. Mater. Sci.* **1995**, *30*, 225. (b) Briggs, D.; Seah, M. P. *Practical Surface Analysis*; J. Wiley & Sons: Chichester, U.K., 1983, and references therein.
(40) Cochran, S. J.; Larkins, F. P. *J. Chem. Soc., Faraday Trans. 1* **1986**, *82*, 1721.
(41) González-Elipe, A. R.; Espinós, J. P.; Fernández, A.; Munuera, G. *Appl. Surf. Sci.* **1990**, *45*, 103.

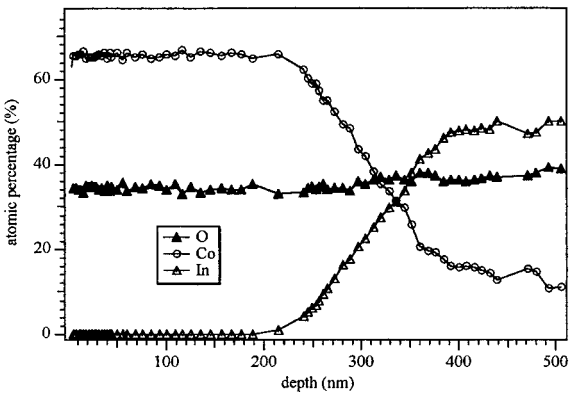

Figure 4. XPS depth profile for sample B (Co_3O_4).

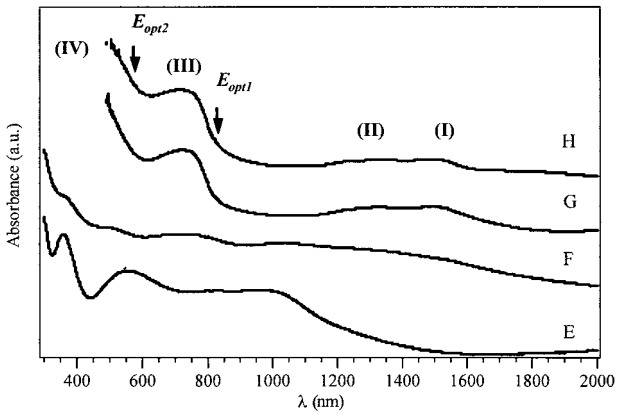

Figure 5. Optical absorption spectra for samples synthesized at 2 mbar pressure. Note that the spectrum of sample E (CoO) is appreciably different from the others.

21.7%), 531.6 (II, 71.4%), and 533.3 (III, 6.9%) eV. While peak I was attributed to the monoxide,[36a] the second and third components were referred to hydroxyl species and adsorbed water, respectively.[42] Even if the presence of hydroxyl groups should cause a shift of about 1 eV in the Co 2p peak BEs,[42c] no such effect was detected. A probable cause relies on the fact that the presence of hydrated species is limited to the outermost layers (see below).

XPS depth profiles showed similar results for all the films. The dependence of O, Co, and In atomic percentages on film thickness for sample B is displayed in Figure 4. The atomic Co and O percentages were almost constant from outer to inner layers, indicative of composition homogeneity. The C 1s signal (not reported in Figure 4) disappeared after mild sputtering, indicating that carbon contamination arose mainly from air exposure and was therefore limited to the outermost part of the layers. After 2′ erosion, the O 1s peak became gradually sharper and its second and third components disappeared, suggesting that they arose mainly from surface contamination. Comparing indium and cobalt depth profiles, an appreciable penetration of the film into the substrate was evidenced. In fact, the coating−substrate interface is quite broad. This effect, which was found for all the analyzed samples, might be ascribed to the relatively high deposition temperatures as well as to the grain nanostructure of the films.

Optical absorption. The obtained Vis−NIR spectra for samples synthesized at $p = 2$ mbar are reported in Figure 5. All the other films exhibited spectral features very similar to those of the samples G and H, in good agreement with the literature data for Co_3O_4. The I band ($\lambda \approx 1520$ nm) was attributed to crystal field $^4A_2(F) \rightarrow {}^4T_1(F)$ transitions in the Co_3O_4 structure.[43] The II signal ($\lambda \approx 1270$ nm) was assigned to an "intervalence" charge-transfer Co(II) ↔ Co(III), representing an internal oxidation−reduction process.[46] Absorptions III ($\lambda \approx 730$ nm) and IV ($\lambda < 500$ nm) were referred to ligand−metal charge transfer (LMCT) events O(−II) → Co(III) and O(−II) → Co(II), respectively).[17,45]

Unlike the previous samples, the spectrum of film E was similar to that reported for CoO.[46] In particular, the band at 357 nm was attributed to LMCT processes O(II) → Co(II), and the absorption centered at 550 nm was ascribed to Co(II) transitions in octahedral crystal field. The optical spectrum of sample F confirmed the presence of both CoO and Co_3O_4.[47]

While the CoO band gap energy (≈5 eV)[36d] is too high to be detected in the Vis−NIR spectra, the Co_3O_4 is a p-type semiconductor[4] and its optical band gap can be obtained from the spectra elaboration. At high frequencies ($\lambda < 500$ nm) the optical absorption is[48]

$$\alpha(h\nu) \propto (h\nu - E_G)^n \qquad (1)$$

where α is the absorption coefficient (cm^{-1}), E_G is the band gap, and the exponent n can take different values depending on the types of electronic transitions in the k-space. The best fitting of eq 1 to the absorption spectra of Co_3O_4 gave $n = 1/2$, meaning the direct allowed transitions for these films.[25] The plots of $(\alpha h\nu)^2$ vs $h\nu$ yielded therefore the band gap extrapolating the linear relationships to zero, i.e., $\alpha = 0$. This procedure allowed to find two optical band gaps ($E_{opt1} \approx 1.5$ eV and $E_{opt2} \approx 2.0$ eV) for all the pure Co_3O_4 samples,[24,49] in agreement with the Co_3O_4 band structure (Figure 6).[24] The valence band has a strong O 2p character, while the main contribution to the conduction band is given by the Co(II) 3d orbitals. The presence of Co(III) centers in Co_3O_4 gives rise to a subband located inside the energy gap. Hence, E_{opt1} correspond to the onset of O(−II) → Co(III) excitations, while E_{opt2} is the "true" energy gap corresponding to interband transitions.

(42) (a) Choudhury, T.; Saied, S. O.; Sullivan, J. L.; Abbot, A. M. *J. Phys. D: Appl. Phys.* **1989**, *22*, 1185. (b) Klingenberg, B.; Grellner, F.; Borgmann, D.; Wedler, G. *Surf. Sci.* **1997**, *383*, 13. (c) Moulder, J. F.; Stickle, W. F.; Sobol, P. E.; Bomben, K. D. *Handbook of X-ray Photoelectron Spectroscopy*; Chastain, J., Ed.; Perkin-Elmer Corp.: Eden Prairie, MN, 1992.

(43) Nkeng, P.; Poillerat, G.; Koenig, J. F.; Chartier, P.; Lefez, B.; Lopitaux, J.; Lenglet, M. *J. Electrochem. Soc.* **1995**, *142*, 1777.

(44) Ruzakowski Athey, P.; Urban, F. K., III; Tabet, M. F.; McGahan, W. A. *J. Vac. Sci. Technol. A* **1996**, *14*, 685.

(45) Belova, I. D.; Roginskaya, Yu. E.; Shifrina, R. R.; Gagarin, S. G.; Plekhanov, Yu. V.; Venevtsev, Yu. N. *Solid State Commun.* **1983**, *47*, 577.

(46) (a) Duran, A.; Fernandez Navarro, J. M.; Casariego, P.; Joglar, A. *J. Non-Cryst. Solids* **1986**, *82*, 391. (b) Orgaz, F.; Rawson, H. *J. Non-Cryst. Solids* **1986**, *82*, 378.

(47) Ashley, J. H.; Mitchell, P. C. H. *J. Chem. Soc. A* **1968**, 2821.

(48) Ramana, C. V.; Hussain, O. M.; Uthanna, S.; Srinivasulu Naidu, B. *Opt. Mater.* **1998**, *10*, *101*.

(49) (a) Murad, W. A.; Al-Shamari, S. M.; Al-Khateeb, F. H.; Misho, R. H. *Phys. Status Solidi A* **1988**, *106*, K143. (b) Schumacher, L. C.; Holzhueter, I. B.; Hill, I. R.; Dignam, M. J. *Electrochim. Acta* **1990**, *35*, 975. (c) Varkey, A. J.; Fort, A. F. *Sol. Energy Mater. Sol. Cells* **1993**, *31*, 277.

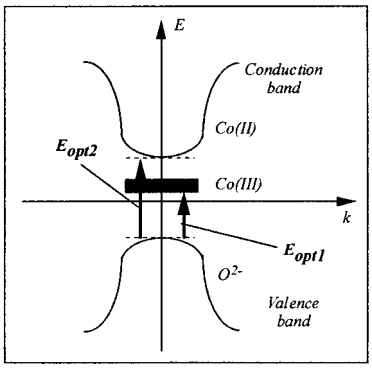

Figure 6. Schematic representation of the band structure of Co_3O_4.[24]

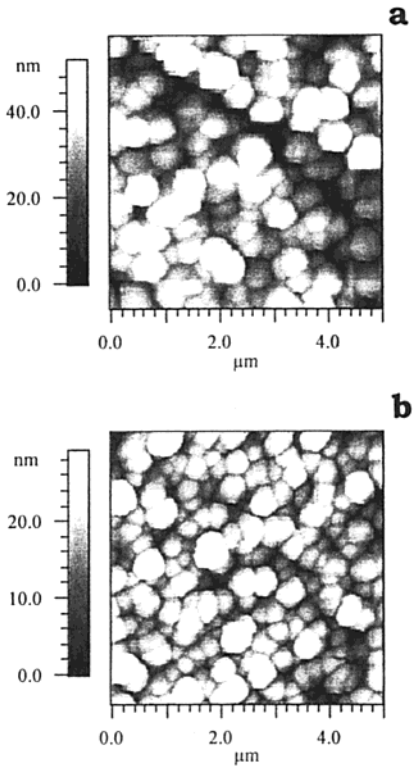

Figure 7. AFM surface micrographs (5 μm × 5 μm): (a) sample B (Co_3O_4); (b) sample E (CoO).

Morphology. Despite the composition and microstructure, the surface morphology was not directly related to the synthesis conditions. As shown in Figure 7, AFM images of samples B (Co_3O_4) and E (CoO) were characterized by the presence of rounded grains (ϕ = 340−580 nm) that can be considered as nanocrystallite aggregations (compare XRD analysis). No appreciable holes or dendrites were detected on the film surfaces. For each deposition pressure, the increase of the substrate temperature corresponded to the increase of the average roughness (from ≈5 to ≈30 nm) and grain size. On the basis of this observation, it was hypothesized the initial formation of many nucleation sites and the subsequent grain growth during the film deposition. Moreover, since the XRD analysis showed no preferential orientation, an "island" (Volmer−Weber) mode was supposed to be the growth mechanism. This observation was in agreement with the results recently obtained in the evaporation of cobalt oxides thin films.[37]

Conclusions

$Co(dpm)_2$ was found to be a suitable and versatile precursor for the CVD of cobalt oxide thin films. It showed a clean decomposition pattern and an appreciable volatility at low temperatures. The main advantage was the possibility of obtaining CoO, CoO + Co_3O_4, and Co_3O_4 thin films controlling the substrate temperature and the reactor pressure. CoO films were obtained on the ITO substrate at temperatures as low as 350 °C and total pressure p = 2 mbar, while Co_3O_4-containing samples were obtained in all the other cases. All the films were nanostructured and their morphological and compositional features could be tailored as indicated by XRD, optical absorption, XPS, and XE-AES measurements. XPS analyses showed that in these synthesis conditions pure and homogeneous cobalt oxide materials were achieved with an effective precursor conversion. Moreover, XPS depth profiles showed an appreciable penetration of the Co oxide layers into the substrate.

Because of the clean and homogeneous nanostructures, the films are of optical quality and do not scatter the visible light;[12] as a perspective, they can be considered as suitable materials for the development of all-solid-state electrochromic devices operating in transmission mode. Nevertheless, the effect of film−substrate intermixing on the usefulness of the layers as electrochromic material has still to be elucidated. To this regard, further work is now in progress and the results will be the subjects of future papers.

Acknowledgment. The authors are grateful to Dr. U. Vettori (CNR-Padova) for the EI-MS spectra of the precursor, to Prof. F. Morandini (Dipartimento CIMA-Università di Padova) for the NMR analysis of the same compound, and to Prof. Paolo Colombo (Dipartimento di Ingegneria Meccanica-Sez. Materiali-Università di Padova) for the XRD measurements. Progetto Finalizzato "Materiali Speciali per Tecnologie Avanzate II" and Programma "Materiali Innovativi Legge 95/95", funded by the CNR, assisted financially the work.

CM001041X